

## Use of viscoelastic polymer sheet as an acoustic control treatment in ceramic tiles to improve sound insertion loss

Piti Sukontasukkul<sup>a,\*</sup>, Khemapat Tontiwattanukul<sup>b</sup>, Avirut Puttiwongrak<sup>c</sup>, Hexin Zhang<sup>d</sup>, Rattapoom Parichatprecha<sup>e</sup>, Cherdasak Suksiripattanapong<sup>f</sup>, Tanakorn Phoo-ngernkham<sup>g</sup>, Thanongsak Imjai<sup>h</sup>, Prinya Chindaprasirt<sup>i,j</sup>

<sup>a</sup> Construction and Building Materials Research Center, Department of Civil Engineering, Faculty of Engineering, King Mongkut's University of Technology North Bangkok, Bangkok, Thailand

<sup>b</sup> Sound and Vibration Engineering Research Group, Department of Mechanical and Aerospace Engineering, King Mongkut's University of Technology North Bangkok, Thailand

<sup>c</sup> Geotechnical and Earth Resources Engineering, School of Engineering and Technology, Asian Institute of Technology, Pathumthani, 12120, Thailand

<sup>d</sup> School of Engineering and the Built Environment, Edinburgh Napier University, Edinburgh, Scotland, United Kingdom

<sup>e</sup> Department of Civil Engineering, School of Engineering, King Mongkut's Institute of Technology Ladkrabang, Bangkok, 10520, Thailand

<sup>f</sup> Department of Civil Engineering, Faculty of Engineering and Technology, Rajamangala University of Technology Isan, Nakhon Ratchasima, 30000, Thailand

<sup>g</sup> Sustainable Construction Material Technology Research Unit, Department of Civil Engineering, Faculty of Engineering and Technology, Rajamangala University of Technology Isan, Nakhon Ratchasima, 30000, Thailand

<sup>h</sup> School of Engineering and Technology, Walailak University, Nakhonsithamarat, 80161, Thailand

<sup>i</sup> Sustainable Infrastructure Research and Development Center, Department of Civil Engineering, Faculty of Engineering, Khon Kaen University, Khon Kaen, 40002, Thailand

<sup>j</sup> Academy of Science, The Royal Society of Thailand, Dusit, Bangkok, 10300, Thailand

### ARTICLE INFO

#### Keywords:

Viscoelastic polymer sheet  
Ceramic tile  
Sound insertion loss  
Damping  
Acoustic control

### ABSTRACT

Ceramic tiles are commonly used in non-structural components of a building such as walls, partitions, floors, and roofs. However, due to their high surface hardness and density, ceramic tiles are not an ideal soundproof material. To improve the sound properties, this study introduced the use of a viscoelastic polymer sheet (VPS) as an acoustic control treatment. The VPS was attached to ceramic tiles in 4 different patterns: X, Cross, Corner, and Strip. The ceramic tiles with VPS were tested for the damping property and sound insertion loss (IL) and then compared to the ones without VPS. Results indicated that the attachment of VPS improved the damping property of the ceramic tiles. All tiles with VPS exhibited higher damping loss indexes than the ones with no VPS. The highest damping loss index of 0.017–0.018 was observed in the specimens with VPS in X and Cross patterns. In the case of IL, the performance of all ceramic tiles was indifferent when tested at sound frequencies smaller than 1000 Hz. At the sound frequencies above 1000 Hz, the best performance was observed in the specimen with VPS in the Cross pattern, followed by X, Strip, and Corner patterns, respectively. This concluded that the use of VPS can improve the damping property of a ceramic tile which also leads to the improvement in sound insertion loss.

### 1. Introduction

One of the most important considerations in the design of a building is to create a comfortable environment for its occupants. There are several factors affecting the level of comfort conditions of a 'home' such as temperature, humidity, noise, air quality, and hygiene. However, the rapid increase in population has increased the demand for land for accommodation and work. It is believed that the human population will

reach 5 billion in the year 2030, and it is expected that about 5.87 million km<sup>2</sup> of land will be needed to convert to urban areas to satisfy such demand [1].

However, not all areas are suitable to support future urban expansion; buildings will be forced to be built taller or closer together in limited spaces. These living conditions can cause negative impacts on home comfort. For example, noise pollution from nearby buildings or vehicles, temperature increase from heat absorbed by the buildings during the daytime [2], poor sanitation conditions [3], and poor indoor

\* Corresponding author.

E-mail addresses: [piti.s@eng.kmutnb.ac.th](mailto:piti.s@eng.kmutnb.ac.th), [piti.kmutnb@gmail.com](mailto:piti.kmutnb@gmail.com) (P. Sukontasukkul).

<https://doi.org/10.1016/j.rineng.2023.100897>

Received 1 November 2022; Received in revised form 25 December 2022; Accepted 13 January 2023

Available online 21 January 2023

2590-1230/© 2023 The Authors. Published by Elsevier B.V. This is an open access article under the CC BY license (<http://creativecommons.org/licenses/by/4.0/>).

**Abbreviation list**

$A(\omega)$	Ratio of Fourier spectrum
$\ddot{X}(\omega)$	Acceleration
$F(\omega)$	Excitation force
$f_n$	Natural frequency
$f_1, f_2$	Frequencies with half power with respected to the natural frequency
$DLR$	Damping loss ratio
$DLF$	Damping loss factor
$IL$	Insertion loss

air conditions [4].

In the case of noise pollution, there are several solutions to control noise nuisance from inside and outside the buildings such as the use of plants and trees to absorb unwanted noises [5], the increase in wall mass or thickness, the reduction of window size to lower noise accepting area [6], and the use of construction materials with high sound insulation. This research deals with the issue related to noise nuisance or pollution in buildings, especially on the novel technique to improve sound properties of construction materials like ceramic tiles.

Construction materials consist of a wide range of materials depending on the purpose of usage. For structural purposes, cement and concrete composite is the most used construction materials on Earth. There are numerous numbers of advanced research in this field. For example, fiber reinforced concrete [7–9], concrete containing phase change materials [10,11], lightweight concrete mixed with crumb rubber [12,13], geopolymer as an alternative cement replacement [14–17], etc. However, when it comes to non-structural parts, ceramic tiles are a type of construction material used in various parts of the building such as roofs, walls, floors, or partitions. In modern construction where walls become thinner and lighter, ceramic wall tiles are used to not only create different appearances but also create spaces and provide protection simultaneously. Floor tiles, on the other hand, are made to be durable, abrasion-resistant, water impervious, easy to clean, and have good aesthetics [18]. In terms of sound properties, ceramic tiles are not an ideal acoustic material [19]. This is because of their high density and hard surface which makes them more difficult to soundproof than other materials like wood, laminate, or rubber.

This research introduces a novel technique to reduce vibration induced by sound incidents by attaching a damper to the surface of ceramic tiles. The technique is expected to improve the damping property of the tile which also leads to an improvement in sound insulation properties (sound insertion loss). In general, the application of damper to reduce product noise has been widely researched and used in appliance and consumer products. There are various kinds of passive dampers being investigated. For example, polymer [20–22], rubber [23–28], cork [29], fiber [30,31], and glass [32,33]. Rubbers generally exhibit better damping capability compared to other materials. They are capable of reducing vibration and sound whereas metals can radiate sound [21,34]. The damping property of rubbers is utilized in a wide range of products like vibration dampers, shock absorbers, bridge bearings, seismic absorbers, rubberized concrete [25–28], etc. Gurgen and Sofuoğlu [29] investigated the improvement in damping properties of cork composite materials in the form of a layer between polymer and shear thickening fluid. They found that the integration of smart materials into cork structures can be used as a passive control system in vibration-damping applications. Kuang and Cuntwell [30] used optical plastic fibers to monitor the damping behavior of fiber composite beams subjected to impact and dynamic loading [31]. Zhang et al. [32] found that the use of polyurethane elastomer synergetic with hollow glass microspheres improves both damping and sound insulation of the material [35].

Although there are several studies on the use of polymer as a passive

damping control material in various applications, not many of them are in decorating construction materials like wall or floor ceramic tiles. This study intended to investigate the matter, add new information to the existing body of knowledge, and examine the possibility of using viscoelastic polymer sheet attachments to improve sound insulation properties. As mentioned earlier, sound insulation properties are important to ceramic tiles used as floor or wall partitions. To create good home comfort, they must have the ability to absorb both vibration and sound from footsteps, falling objects, external voices, etc. In this study, the viscoelastic polymer sheet (VPS) was used as a passive sound and damping control material attached to ceramic tiles in several patterns. The experimental series included a damping test and sound insertion loss.

## 2. Experimental process

### 2.1. Materials

Materials used in this study consisted of commercial-type ceramic tiles for wall partitions or floors applications with the dimensions of  $300 \times 300 \times 8$  mm (width x length x thickness) with properties given in Table 1, and viscoelastic polymer sheets (VPS) (Butyl rubber compound type) with the dimensions of  $100 \times 1$  mm (width x thickness) with the properties as shown in Table 2.

### 2.2. VPS patterns

The VPS sheets were attached to the bottom surface of a ceramic tile with the patterns as shown in Table 3. The selected patterns were determined by the mode shapes from the damping vibration test (more details are described in the Results and Discussion section).

### 2.3. Experimental series

The experimental series consisted of a vibrating damping test (ASTM E756) [36] and sound insertion loss using a sound insertion loss testing chamber constructed at the Department of Civil Engineering, King Mongkut's University of Technology North Bangkok.

#### 2.3.1. Vibration damping test

The objective of the test was to measure the mode shapes, natural frequencies, and damping loss factors of the specimens. The equipment consisted of a data acquisition unit (NI USB-4431), an accelerometer (Bruel & Kjaer 4507B), and a force transducer (PCB 208C01 response rate of 0.01–36,000 Hz) with specification as shown in Table 4.

The testing process began by cleaning and drying the surface of the test specimen, dividing the testing surface into 36 square patches of  $50 \times 50$  mm (Fig. 1). An accelerometer was securely attached at the center of the top left corner square. The specimen was then placed on a light damp material, e.g. sponge. The boundary condition as Free-Free-Free-Free is considered. The impact test was performed by impacting the hammer at the center of each square. The signals from the hammer and accelerometer were recorded and later processed using a Matlab script to calculate the frequency response function (FRF). The test continued until all squares were hit by the hammer. Using the obtained natural

**Table 1**  
Properties of ceramic tile.

Specification	
Breaking strength (MPa)	35–40
Mohr scale hardness	6–7
Thickness (mm)	8
Water absorption (%)	0.2
Stain resistance	Class 5
Coefficient of friction	R9

**Table 2**  
Properties of viscoelastic polymer sheet.

Specification	
Density (g/cm <sup>3</sup> )	1.5
Thickness (mm)	1
Thickness (mm)	100
Service temperature (°C)	-30 to 40
Tensile strength (N/25 mm)	124
Elongation at break (%)	100

frequencies and mode shapes, the damping was determined using the method described below.

It must be noted that the frequency response was introduced in this work in order to evaluate the damping ratio of the specimen. By definition, the frequency response is the ratio between acceleration over force, which is measured by accelerometer and force transducer respectively. It can be said that the response is normalized by the magnitude of the excitation force already. Thus, the evaluation of the damping is based on the acceleration per unit force.

Based on ASTM E756, once the FRF of a plate is obtained, the half-power method is applied to determine the damping ratios. Fig. 2a shows an FRF of a square plate ( $A(\omega)$ ) which is the ratio of the Fourier spectrum of the acceleration signal  $\ddot{X}(\omega)$  to excitation force  $F(\omega)$  (Eq. (1))

$$A(\omega) = \frac{\ddot{X}(\omega)}{F(\omega)} \tag{1}$$

The FRF can be dissected into a series of single-degree freedom systems. Thus, the damping ratio is obtained by eliminating each peak (Fig. 2b) to determine the half-power frequencies,  $f_1$  and  $f_2$ , which are the half-power frequencies with respect to the peak (natural frequency,  $f_n$ ). Using the obtained half-power frequencies, the damping loss ratio (DLR) can be computed using Eq. (2).

$$DLR = \frac{(f_2 - f_1)}{2f_n} \tag{2}$$

The damping loss factor (DLF) can then be obtained using the relationship in Eq. (3).

$$DLF = 2DLR = \frac{(f_2 - f_1)}{f_n} \tag{3}$$

The DLF indicates the ability of a structure to dissipate energy. Structural systems with higher DLF allow vibrations to decay faster.

2.3.2. Sound insertion loss test

Insertion Loss (IL) refers to the reduction of noise level at a given location due to the placement of a noise control device in the sound path between the sound source and that location. The objective of the Sound Insertion Loss (SIL) test is to determine the ability of a noise control

device to reduce the noise level from the sound source propagating through a given path. In this study, the ceramic tile serves as a passive noise control device.

The test was carried out using a sound insertion loss chamber constructed at the Department of Civil Engineering, KMUTNB (Fig. 3). The chamber with dimensions of 700 × 2000 × 800 mm (width x height x depth) consisted of two rooms: absorptive room and reverberation room. The absorptive room was a rectangular-shaped room constructed with interior walls lining highly absorptive materials and equipped with an intensity probe. The intensity probe consisted of 2 microphones and a 12-mm spacer (Fig. 4). The reverberation room was constructed with nonparallel walls and equipped with a speaker (working range of 50–20000 Hz) located at the corner of the room.

The testing steps are as follows: 1) placing a specimen at the opening between the absorptive and reverberation rooms, 2) filling up voids between the specimen and the support with greasy gel, 3) adjusting the intensity probe to have a distance of 150 mm from the specimen, 4) playing sounds from the speaker with the frequency range from 20 to 20000 Hz, 5) measuring the sound intensity, and 6) removing the specimen and measuring the sound intensity of the box with an opening.

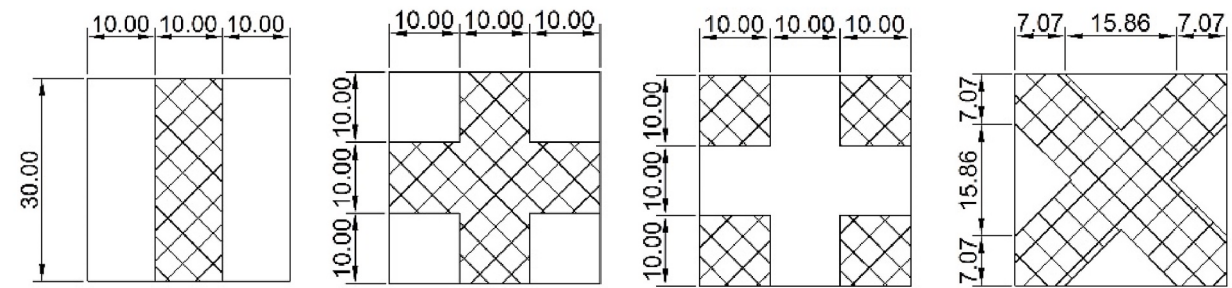
The sound insertion loss can be calculated using the following

**Table 4**  
Specification of equipment used in damping vibration test.

Data acquisition unit (NI USB-4431)	
4 analog input channels ±10 V, 102.4 kS/s simultaneous sampling rate	
1 analog output channels ±3.5 V, 96 kS/s update rate	
24-bit resolution	
Software-selectable IEPE signal conditioning (0–2.1 mA)	
NIST-traceable calibration	
Accelerometer (Bruel & Kjaer 4507B)	
Freq. range: 0.3–6000 Hz	
Temperature: 54 – 121 °C	
Weight: 4.8 g	
Sensitivity: 10 mV/ms <sup>-2</sup>	
Residual Noise Level in Spec Freq Range (RMS): ±350 µg	
Maximum Operational Level (peak): 70 g	
Resonance frequency: 18 kHz	
Maximum Shock Level (±peak): 5000 g	
Force transducer (PCB 208C01)	
Measurement Range: 10 lb (0.04448 kN)	
Sensitivity: (±15%)500 mV/lb (112,410 mV/kN)	
Low-Frequency Response: (–5%) 0.01 Hz	
Upper-Frequency Limit: 36,000 Hz	
Temperature Range: 65 to +250 °F (–54 to +121 °C)	
Mounting Thread: 10–32 Female	

**Table 3**  
VPS patterns of the ceramic tile.

Designation	Strip	Cross	Corner	X
Abbreviation	S	Cr	Cn	X

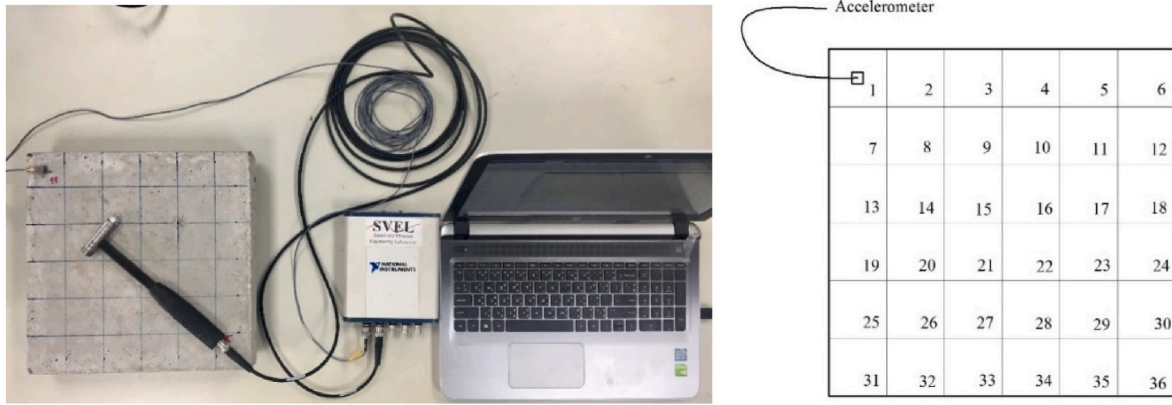


Fig. 1. Test equipment and installation of the sensor.

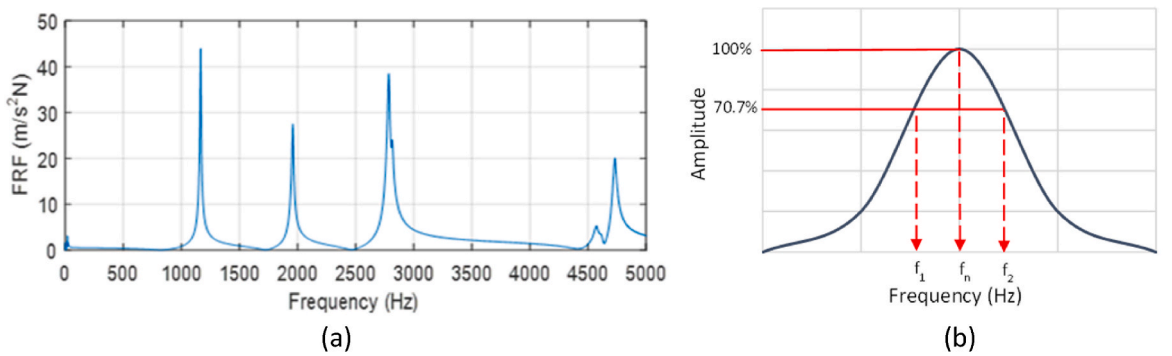


Fig. 2. Frequency response function (FRF).

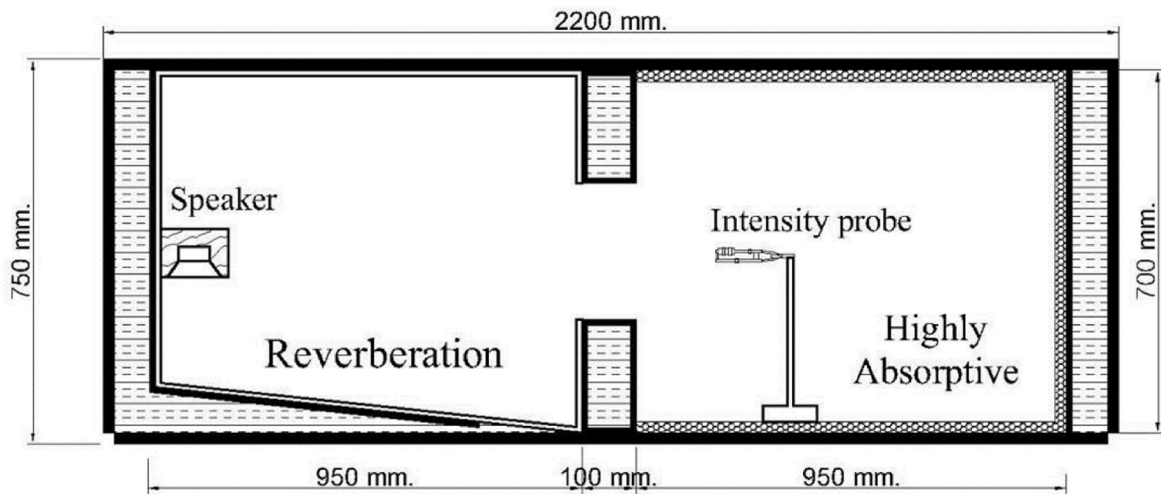


Fig. 3. Sound insertion loss chamber.

equation:

$$IL = I_2 - I_1 \tag{4}$$

where  $IL$  is the insertion loss or ability to reduce noise (dB),  $I_1$  is the sound intensity with the specimen (dB), and  $I_2$  is the sound intensity without the specimen (opening) (dB).

### 3. Results and discussion

#### 3.1. Vibration damping test

Results from the vibration damping test consisted of 2 parts: vibration mode shape and damping loss factor.

##### 3.1.1. Vibration mode shape

The results on the vibration mode shape are shown in Fig. 4. Based on the current test setup, 14 mode shapes were obtained. In general, the

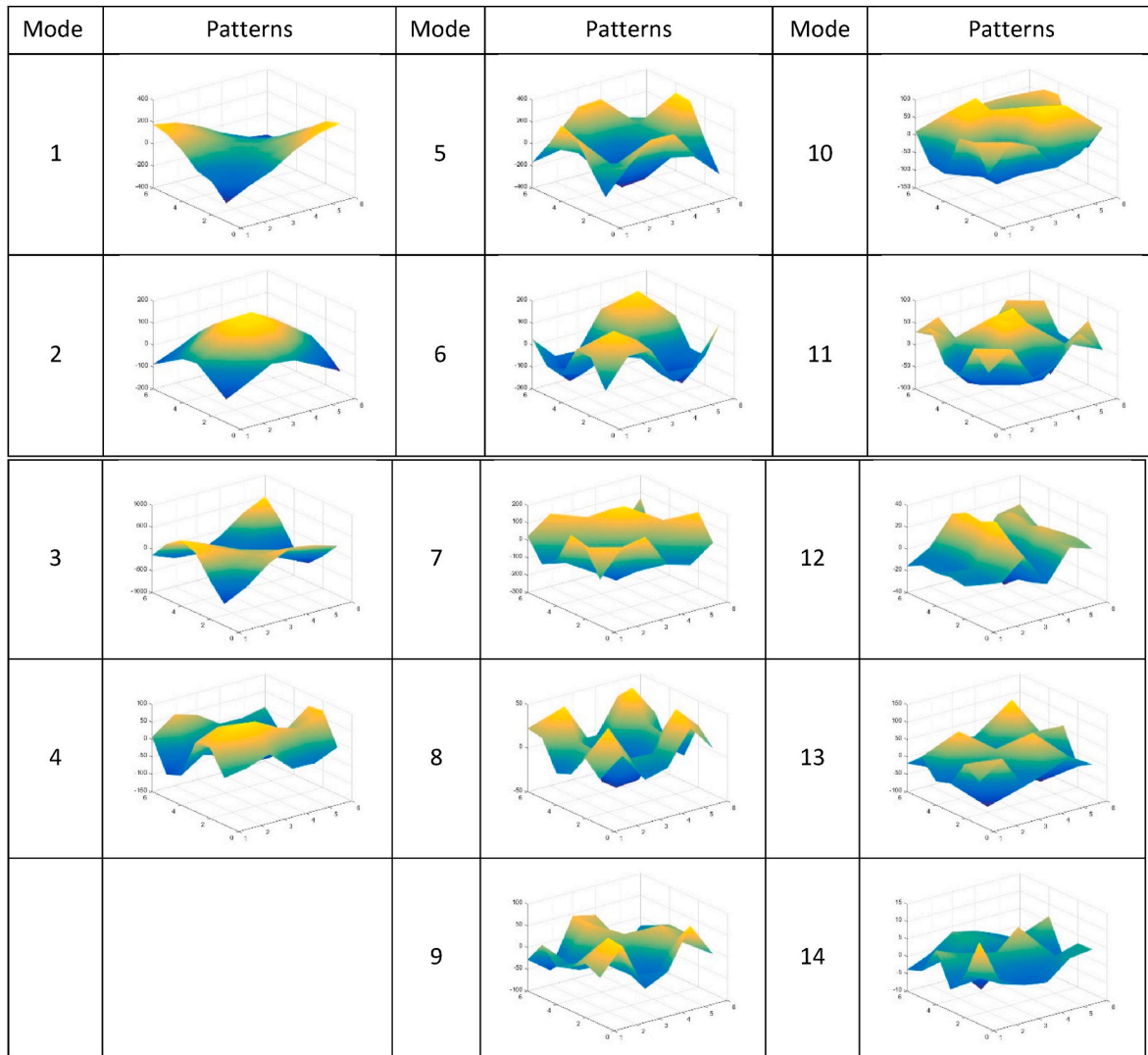


Fig. 4. Vibration mode shape.

mode shape can be defined as a way of vibrating, a pattern of vibration of the system, or a structure that has several points with different amplitudes of deflection when subjected to vibration at the natural frequency.

Based on the obtained results, it was found that different vibration modes gave different vibrating patterns and amplitudes. However, the locations where the maximum vibration occurred were observed repeatedly at the corners, center, and middle strip. These locations were used in determining the patterns of the VPS sheets attached to the specimen.

3.1.2. Damping loss factor

The damping loss factor (DLF) of the ceramic tile without the VPS attachment was around 0.008  $\eta$ . With the VPS sheet, the DLF increased to about 0.012–0.018 depending on the VPS pattern. The X-pattern was found to exhibit the highest DLF followed by Cross, Strip, and Corner, respectively (Fig. 5).

Consider the 14 mode shapes illustrated in 3.1.1, the vibration at the center of the tile was found in 9 out of 14 mode shapes. Since the center of the tile is the area with the greatest number of vibration appearances and also since the corner specimen was the only type with no VPS cover in this area, this allowed more vibration to occur in the corner specimen and hence lower the DLF (0.012  $\eta$ ). As for the other three patterns (strip, cross, and X) which had VPS covering the center of the tile, this limited

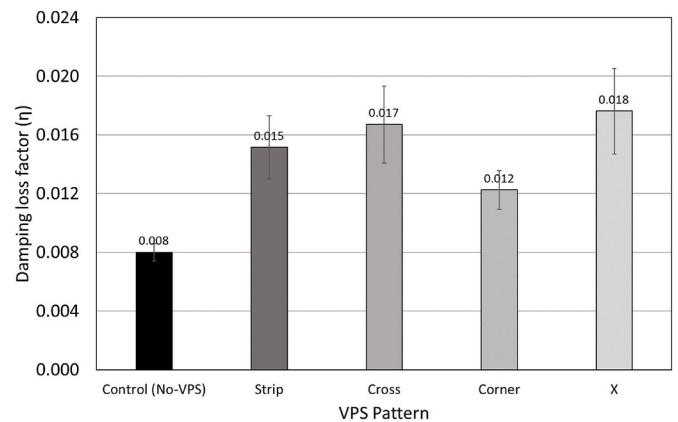


Fig. 5. Damping loss factor of ceramic tiles attaches with VPS at different patterns.

the vibration to occur and thus increased the DLF (0.015–0.018  $\eta$ ).

3.2. Sound insertion loss

The test was carried out based on ASTM E-413 [37]. The sound

insertion loss within the frequency range of 125–8000 Hz was determined from the measured sound intensity. The results on sound intensity with and without a specimen ( $I_1$  and  $I_2$ ) at different frequency ranges from 125 to 8000 Hz are given in Table 5. Both  $I_1$  and  $I_2$  were found to depend on the frequency of the sound that is being used during the measurement. In general,  $I_2$  is higher than  $I_1$  because there was no specimen blocking the opening, and hence, more sounds were allowed to travel from the reverberation to the absorption room. The intensity level with an opening ( $I_2$ ) was found in the range of 47–66 dB depending on the sound frequency. With the specimen placed at the opening blocking the sound path, less sound can pass to the absorption room which caused a low sound intensity level. The  $I_1$  of the control tile (No-VPS) was found to range from 33 to 42 dB, while in the specimen with VPS, the  $I_1$  was slightly lower than the control tile with intensity ranging from 33 to 40 dB depending on the sound frequency.

Using Eq. (4) and the results on sound intensity, the insertion loss (IL) can be calculated, and the results are shown in Fig. 6. In general, sound insertion loss of material depends strongly on the sound frequency used in the test. At a low frequency from 125 to 500 Hz, there was almost no difference in sound insertion loss found between each type of specimen. The IL was observed in the range of 7.1–26.9 dB. With the increase in sound frequency to a medium range (500–2000 Hz), the differences in IL between different types of tiles were observed at frequencies higher than 1000 Hz. At sound frequencies higher than 1000 Hz, the ceramic tiles with VPS appeared to perform better than those without VPS. The cross pattern showed the highest IL of 31.6–32.5 dB followed by X-pattern (29.7–31.9 dB), strip pattern (27.6–29.8 dB), corner pattern (24.6–32 dB), and No-VPS (22–31 dB), respectively. At a high-frequency range (higher than 2000 Hz), the VPS tiles were found to outperform the no VPS tiles in every sound frequency. The maximum IL of 39.8 dB was observed in the VPS tile with a cross-pattern at the frequency of 5000 Hz While the lowest IL of 28.4 was observed in the no VPS tile at the sound frequency of 2000 Hz. All VPS tiles exhibited their highest IL at the frequency of 5000 Hz.

#### 4. Conclusion

Based on the experimental results, the following conclusion can be drawn.

- A viscosity polymer sheet can be used as a passive damper in ceramic tile to reduce vibrations from the inserted impulsive force. The effectiveness of VPS depends strongly on the pattern being used. For passive vibration control, the best performance was the X pattern followed by the Cross, Strip, Corner, and No VPS, respectively.
- The use of VPS attachment can not only reduce vibration but also lead to an improvement in sound insertion loss (IL). The IL of all ceramic tiles attached to VPS sheets was found to be higher than those without VPS sheets. Like the case of damping, the IL depended strongly on the sound frequency and VPS pattern. At a low-frequency range, the performance of all tiles was in a similar range. At a high frequency of over 1000 Hz, all the tiles with VPS performed better than those with no VPS. Comparing the VPS tiles, the IL ranging from the highest to lowest is Cross, X, Strip, and Corner pattern, respectively. The results thus indicate that the tiles with Cross and X patterns performed considerably well in b The improvement in damping properties and sound insertion loss can be a benefit to the buildings depending on the type of application.
- In terms of applications, in the case of floor component, the high damping ratio of the VPS tiles can reduce the vibration induce to the floor from the impact of falling objects. However, in terms of sound absorption, since most in-house sound frequencies are in lower ranges, the use of VPS ceramic tiles in floor application may not be very effective. As for the wall partition application, the use of VPS ceramic tiles may be beneficial when use as exterior walls because sounds from outside the building comes in wide range and could be in high pitch ranges.
- Recommendation for future work includes the analysis on the role and mechanism of VPS patterns in improving damping properties.

#### Credit author statement

Piti Sukontasukkul Main supervisor, Conceptual design, First draft editing, Final draft review, Funding. Khemapat Tontiwattanakul Research design, Main investigator, Data collection, Resource. Avirut Puttiwongrak Investigator, Research assistant, Validate. Hexin Zhang Validate, Final draft editing. Rattapoom Parichatprecha Validate, Cherdasak Suksiripattanapong Validate. Tanakorn Phoo-ngernkham Validate. Thanongsak Imjai Validate. Prinya Chindaprasirt Supervisor,

**Table 5**  
Sound intensity levels at different sound frequency levels.

Low frequency range		Sound intensity (dB)						
Frequency (Hz)		125	160	200	250	315	400	500
$I_2$		55.3	52.8	63.4	53.6	47.7	50.4	52.0
$I_1$ (No-VPS)		33.0	25.9	41.6	38.7	40.5	38.7	26.7
$I_1$ (Strip)		33.0	26.7	39.1	37.2	40.6	38.8	26.7
$I_1$ (Cross)		33.2	26.6	39.4	37.0	40.2	38.3	26.4
$I_1$ (Corner)		33.3	25.9	40.9	37.4	40.5	38.2	26.7
$I_1$ (X)		33.5	26.4	37.0	36.7	40.4	38.2	26.6
Medium frequency range		Sound intensity (dB)						
Frequency (Hz)		630	800	1000	1250	1600	2000	
$I_2$		56.7	63.0	65.1	63.9	61.8	60.3	
$I_1$ (No-VPS)		30.4	37.1	34.1	41.9	34.3	31.9	
$I_1$ (Strip)		30.7	36.3	35.3	36.3	32.1	30.5	
$I_1$ (Cross)		30.5	36.1	33.5	33.9	30.5	27.8	
$I_1$ (Corner)		30.5	37.3	33.1	39.3	32.4	29.6	
$I_1$ (X)		30.4	35.9	33.9	34.2	30.9	28.4	
High frequency range		Sound intensity (dB)						
Frequency (Hz)		2500	3150	4000	5000	6300	8000	
$I_2$		62.0	65.1	64.3	66.2	65.8	64.7	
$I_1$ (No-VPS)		32.7	34	32.1	35.5	34.7	35.6	
$I_1$ (Strip)		31.9	31.8	30.7	30.8	33.9	35.0	
$I_1$ (Cross)		27.1	29.1	26.4	26.4	32.5	34.0	
$I_1$ (Corner)		30.4	30.7	29.5	30.4	31.8	33.6	
$I_1$ (X)		29.2	27.8	29.6	28.8	33.6	34.1	

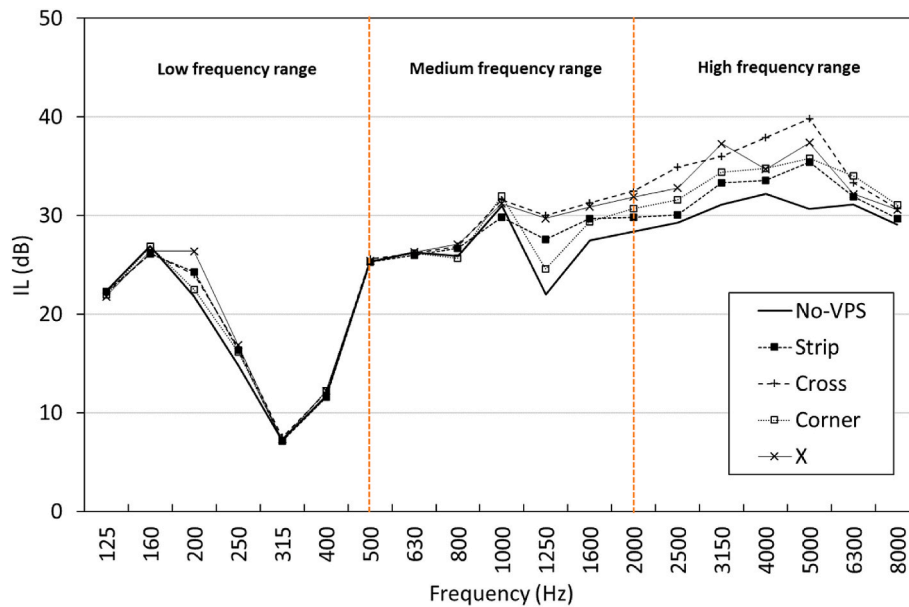


Fig. 6. Sound insertion at different sound frequencies.

First draft review, Final draft review.

#### Declaration of competing interest

The authors declare that they have no known competing financial interests or personal relationships that could have appeared to influence the work reported in this paper.

#### Data availability

No data was used for the research described in the article.

#### Acknowledgment

This research is funded by the National Science Research and Innovation Fund (NSRF) and King Mongkut's University of Technology North Bangkok (KMUTNB) under contract no. KMUTNB-FF-66-02.

#### References

- [1] K.C. Setoa, B. Güneralpa, L.R. Hutyra, Global forecasts of urban expansion to 2030 and direct impacts on biodiversity and carbon pools, *Proc. Natl. Acad. Sci. USA* 109 (40) (2012) 16083–16088.
- [2] S. May, ARE CITY BUILDINGS MAKING US HOTTER?, 2013. Retrieved from, <http://www.premierguarantee.com/resource-hub/are-city-buildings-making-us-hotter/>.
- [3] United Foresight, Module 4: unique urban sanitation issues (n.d.) Retrieved from: <http://www.uniteforsight.org/urban-health/module4>.
- [4] United State Environmental Protection Agency, Introduction to Indoor Air Quality, Research and Development, 2022. Retrieved from, <https://www.epa.gov/indoor-air-quality-iaq/introduction-indoor-air-quality#health>.
- [5] J. Carroll, Planting Noise Blockers: Best Plants for Noise Reduction in Landscapes, 2021. Retrieved from, <https://www.gardeningknowhow.com/special/spaces/noise-reduction-plants>.
- [6] The Constructor, Construction techniques in acoustic planning of a building, (n.d.), Retrieved from, <https://theconstructor.org/building/construction-techniques-in-acoustic-planning-of-a-building/14976/>.
- [7] W. Wongprachum, M. Sappakittipakorn, P. Sukontasukkul, P. Chindaprasirt, N. Banthia, Resistance to sulfate attack and underwater abrasion of fiber reinforced cement mortar, *Construct. Build. Mater.* 189 (2018) 686–694, <https://doi.org/10.1016/j.conbuildmat.2018.09.043>.
- [8] P. Sukontasukkul, S. Mindess, N. Banthia, Properties of confined fibre-reinforced concrete under uniaxial compressive impact, *J. Cem. Concr. Res.* 35 (1) (2005) 11–18, <https://doi.org/10.1016/j.cemconres.2004.05.011>.
- [9] P. Sukontasukkul, S. Mindess, The shear fracture of concrete under impact loading using end confined beams, *Mater. Struct.-Spec. Iss. Concr. Sci. Eng. RILEM* 36 (260) (2003) 372–378, <https://doi.org/10.1007/BF02481062>.
- [10] P. Uthaichotirat, P. Sukontasukkul, P. Jitsangiam, C. Suksiripattanapong, V. Sata, V., P. Chindaprasirt, Thermal and sound properties of concrete mixed with high porous aggregates from manufacturing waste impregnated with phase change material, *J. Build. Eng.* 29 (2020), 101111, <https://doi.org/10.1016/j.jobbe.2019.101111>.
- [11] P. Sukontasukkul, E. Intawong, P. Premanoch, P. Chindaprasirt, Use of paraffin impregnated lightweight aggregates to improve thermal properties of concrete panels, *Mater. Struct.* 49 (5) (2016) 1793–1803, <https://doi.org/10.1617/s11527-015-0612-8>.
- [12] C. Chaikaew, P. Sukontasukkul, U. Chaisakulkiet, V. Sata, P. Chindaprasirt, Properties of concrete pedestrian blocks containing crumb rubber from recycle waste tyres reinforced with steel fibres, *Case Stud. Constr. Mater.* 11 (2019), e00304, <https://doi.org/10.1016/j.cscm.2019.e00304>.
- [13] P. Sukontasukkul, S. Jamnam, M. Sappakittipakorn, N. Banthia, Preliminary study on bullet resistance of double-layer concrete panel made of rubberized and steel fiber reinforced concrete, *Mater. Struct.* 47 (1) (2014) 117–125, <https://doi.org/10.1617/s11527-013-0049-x>.
- [14] A. Wongsu, A. Siriwattanakarn, P. Nuaklong, V. Sata, P. Sukontasukkul, P. Chindaprasirt, Use of recycled aggregates in pressed fly ash geopolymer concrete, *Environ. Prog. Sustain. Energy* 39 (2020), e13327, <https://doi.org/10.1002/ep.13327>.
- [15] P. Sukontasukkul, P. Chindaprasirt, P. Pongsopha, T. Phoo-Ngernkham, W. Tangchirapat, W., N. Banthia, Effect of fly ash/silica fume ratio and curing condition on mechanical properties of fiber-reinforced geopolymer, *J. Sustain. Cement-Based Mater.* 9 (4) (2020) 218–232, <https://doi.org/10.1080/21650373.2019.1709999>.
- [16] S. Dueramae, W. Tangchirapat, P. Chindaprasirt, C. Jaturapitakkul, P. Sukontasukkul, Autogenous and drying shrinkages of mortars and pore structure of pastes made with activated binder of calcium carbide residue and fly ash, *Construct. Build. Mater.* 230 (2020), 116962, <https://doi.org/10.1016/j.conbuildmat.2019.116962>.
- [17] P. Sukontasukkul, N. Nontiyutisirikul, S. Songpiriyakij, K. Sakai, P. Chindaprasirt, Use of phase change material to improve thermal properties of lightweight geopolymer panel, *Mater. Struct.* 49 (11) (2016) 4637–4645, <https://doi.org/10.1617/s11527-016-0812-x>.
- [18] E. Monfort, A. Mezquita, E. Vaquer, I. Celades, V. Sanfeliix, A. Escrig, 8.05 - ceramic manufacturing processes: energy, environmental, and occupational health issues, in: Saleem Hashmi, Gilmar Ferreira Batalha, Chester J. Van Tyne, Bekir Yilbas., *Comprehensive Materials Processing*, vol. 8, Elsevier, 2014, pp. 71–102, <https://doi.org/10.1016/B978-0-08-096532-1.00809-8>.
- [19] S.L. Poirier, Soundproofing a Bathroom Adequately: Ceramic Tile or Vinyl Flooring?, 2020. Retrieved from, <https://www.acousti-tech.com/en/blog/de-tail/soundproofing-a-bathroom-adequately-ceramic-tile-or-vinyl-flooring-11181>.
- [20] P. Butaud, E. Foltete, M. Ouisse, Sandwich structures with tunable damping properties: on the use of Shape Memory Polymer as viscoelastic core, *Compos. Struct.* 153 (2016) 401–408, <https://doi.org/10.1016/j.compstruct.2016.06.040>.
- [21] V.G. Geethamma, R. Asaletha, N. Kalarikkal, N., Vibration and sound damping in polymers, *Resonance* 19 (2014) 821–833, <https://doi.org/10.1007/s12045-014-0091-1>.
- [22] J.A. Grates, D.A. Thomas, E.C. Hickey, L.H. Sperling, Noise and vibration damping with latex interpenetrating polymer networks, *J. Appl. Polym. Sci.* 19 (1975) 1731–1743, <https://doi.org/10.1002/app.1975.070190623>.
- [23] R.D. Kornbluh, H. Prahlah, R. Pelrine, S. Stanford, M.A. Rosenthal, P.A. von Guggenberg, Rubber to rigid, clamped to undamped: toward composite materials

- with wide-range controllable stiffness and damping, in: Proc. SPIE 5388, Smart Structures and Materials 2004: Industrial and Commercial Applications of Smart Structures Technologies, 2004, <https://doi.org/10.1117/12.548971>.
- [24] C. Liu, J.F. Fan, Y.K. Chen, Design of regulable chlorobutyl rubber damping materials with high-damping value for a wide temperature range, *Polym. Test.* 79 (2019), 106003, <https://doi.org/10.1016/j.polymertesting.2019.106003>.
- [25] P. Pongsopha, P. Sukontasukkul, H. Zhang, S. Limkatanyu, Thermal and acoustic properties of sustainable structural lightweight aggregate rubberized concrete, *Res. Eng.* 13 (2022), 100333, <https://doi.org/10.1016/j.rineng.2022.100333>.
- [26] P. Pongsopha, P. Sukontasukkul, B. Maho, D. Intarabut, T. Phoo-ngernkham, S. Hanjitsuwan, D. Choi, S. Limkatanyu, Sustainable rubberized concrete mixed with surface treated PCM lightweight aggregates subjected to high temperature cycle, *Construct. Build. Mater.* 303 (2021), 124535, <https://doi.org/10.1016/j.conbuildmat.2021.124535>.
- [27] B. Maho, S. Sukontasukkul, S. Jamnam, E. Yamaguchi, K. Fujikake, N. Banthia, Effect of rubber insertion on impact behavior of multilayer steel fiber reinforced concrete bulletproof panel, *Construct. Build. Mater.* 216 (2019) 476–484, <https://doi.org/10.1016/j.conbuildmat.2019.04.243>.
- [28] P. Sukontasukkul, S. Jamnam, K. Rodsin, N. Banthia, Use of rubberized concrete as a cushion layer in bulletproof fiber reinforced concrete panels, *Construct. Build. Mater.* 41 (2013) 801–811, <https://doi.org/10.1016/j.conbuildmat.2012.12.068>.
- [29] S. Gürgeç, M.A. Sofuoğlu, Smart polymer integrated cork composites for enhanced vibration damping properties, *Compos. Struct.* 258 (2021), 113200, <https://doi.org/10.1016/j.compstruct.2020.113200>.
- [30] K.S.C. Kuang, W. J. Cantwell, The use of plastic optical fibres and shape memory alloys for damage assessment and damping control in composite materials, *Meas. Sci. Technol.* 14 (2003) 1305.
- [31] P. Sukontasukkul, S. Mindess, The shear fracture of concrete under impact loading using end confined beams, *Mater. Struct.* 36 (2002) 372–378, <https://doi.org/10.1007/BF02481062>.
- [32] Z. Zhang, H. Jiang, R. Li, et al., High-damping polyurethane/hollow glass microspheres sound insulation materials: preparation and characterization, *J. Appl. Polym. Sci.* 138 (2021), e49970, <https://doi.org/10.1002/app.49970>.
- [33] F.W. Al-Awabdeh, M.J. Al-Kheetan, Y.S. Jweihan, H. Al-Hamaiedeh, S.H. Ghaffar, Comprehensive investigation of recycled waste glass in concrete using silane treatment for performance improvement, *Res. Eng.* 16 (2022), 100790, <https://doi.org/10.1016/j.rineng.2022.100790>.
- [34] M. Graf, T. Lanckenau, Viscous damping exciting friction-induced vibration in pin-on-disk systems, *Res. Eng.* 12 (2021), 100299, <https://doi.org/10.1016/j.rineng.2021.100299>.
- [35] I. Veza, Z. Zainuddin, N. Tamaldin, M. Idris, I. Irianto, I.M.R. Fattah, Effect of palm oil biodiesel blends (B10 and B20) on physical and mechanical properties of nitrile rubber elastomer, *Res. Eng.* 16 (2022), 100787, <https://doi.org/10.1016/j.rineng.2022.100787>.
- [36] ASTM E756-05 Standard Test Method for Measuring Vibration-Damping Properties of Materials, ASTM International, West Conshohocken, PA, 2005.
- [37] ASTM E413-22 Classification for Rating Sound Insulation, ASTM International, West Conshohocken, PA, 2022.